Catalysis Letters 65 (2000) 43–48

Structures and performance of Pd–Mo–K/Al_2O_3 catalysts used for mixed alcohol synthesis from synthesis gas

Zhong-rui Li [a], Yi-lu Fu [a,*], Ming Jiang [a], Ming Meng [a], Ya-ning Xie [b], Tian-dou Hu [b] and Tao Liu [b]

[a] *Department of Chemical Physics, University of Science and Technology of China, Hefei 230026, PR China*
E-mail: fulin@ustc.edu.cn
[b] *Beijing Synchrotron Radiation Facility, Beijing 100039, PR China*

Received 25 October 1999; accepted 14 January 2000

The structures of the palladium-modified Mo–K/Al_2O_3 catalyst samples were characterized by the XRD, LRS, and EXAFS techniques and correlated to the catalytic properties of the samples for alcohol synthesis from synthesis gas. It is found that in the oxidic palladium-modified samples a strong interaction of the palladium modifier with the supported K–Mo–O species occurs. This interaction leads to a decrease in the size of the molybdenum species and stabilization of the cationic palladium species on the samples during sulfidation. Upon sulfidation, the sulfided molybdenum species in the palladium-free sample is mainly present as large patches of MoS_2-like slabs with their basal sulfur planes interacting with the support surface. With the modification of palladium to the samples, the supported MoS_2-like species becomes highly dispersed as revealed by the decrease in the average size of the sulfided molybdenum species. The interaction of the palladium species with the molybdenum component may cause the basal planes of the MoS_2-like species to become oriented perpendicular to the support surface due to favorable bonding of the MoS_2 edge planes to the support through Mo–O–Al bonds. In comparison with the sulfided Pd-free sample, the properties of the Pd-modified samples for alcohol synthesis from synthesis gas are much improved, which most probably results from the synergic interaction of the palladium with the molybdenum species that gives rise to the appearance of the active sites.

Keywords: sulfided Pd–Mo–K/Al_2O_3 catalysts, structure characterizations, mixed alcohol synthesis

1. Introduction

During the past 10 years, there has been considerable interest in developing processes for the synthesis of higher alcohols (C_2 and higher) from syngas for use as additives to gasoline (usually 2–5 wt%) to reduce air pollution and increase the octane number [1]. The need for an octane enhancer stems from the phasing out of lead from the gasoline and a push for higher levels of pollution control. The presence of oxygenate additives in the fuel allows for combustion to proceed to a greater extent, such as methanol as an additive to gasoline. Combining a mixture of C_2–C_5 alcohols with methanol helps overcome the problem of methanol phase separation with water and lowers the overall vapor pressure of the fuel.

It is generally agreed that there are at least two main requirements for an active alcohol-synthesis catalyst [2]. First, the catalyst should adsorb CO without dissociating the molecule. Second, the catalyst should adsorb H_2 dissociatively [3]. The first requirement of nondissociative CO adsorption is thought to be the more critical and complex of these catalyst properties. While nondissociation of CO is desired, the CO should also be activated sufficiently that H_2 could be attached to both ends of the molecule. These CO adsorption properties are generally provided by metals having atomic configurations with nearly or totally filled d-shells [4]. For the current most active catalyst, Cu provides this property; other active metals, such as Rh, Pd, and Pt, fall within this category [5]. The oxidation state of these metals should strongly influence their d character and, therefore, their reactivity.

Pd/SiO_2 catalysts with and without promoters for methanol synthesis have been previously studied [6]. With partially contradictory conclusion, Lunsford et al. [7] concluded that Pd structural effects play an important role in the activity of the catalyst, since catalysts with small Pd crystallites produce methanol while larger crystallites produce methane. Such structural effects can be induced by different grades of silica support. On the other hand, Ponec et al. [8] believe that electronic factors are more important and ionic Pd sites are the centers for CO activation. The number of such sites is presumably increased by the presence of alkali metals. The effect of alkali metals such as Li appears to be more complex [9]. Whatever the nature of the active centers, the addition of basic metals as well as the use of basic support [10] promotes reactivity.

By several years of research work, our lab succeeded in preparing a new kind of sulfided K–Mo/Al_2O_3 catalyst, which showed relatively high activity and selectivity for mixed alcohols synthesis. Under the reaction conditions of 658 K, 14.0 MPa and 11 000 h^{-1}, the alcohols space–time yield (STY) was up to 416.7 ml l^{-1} h^{-1} and alcohols selectivity was 82%, but methanol content in the alcohols product was relatively high [11]. Increasing the content of C_{2+} alcohols is desirable from the practical point of view.

* To whom correspondence should be addressed.

So far, sulfided molybdenum-based catalysts modified by palladium used for alcohol synthesis have hardly been reported in literature. In the present work, a series of sulfided Pd–Mo–K/Al_2O_3 catalyst samples with different palladium loadings has been prepared and investigated for the synthesis of mixed alcohols from synthesis gas. The interaction between the palladium and molybdenum components and its effect on dispersion of the supported molybdenum species are elucidated based upon the characterizations by using a variety of techniques as mentioned below. The correlation between the catalyst structures and their catalytic properties for alcohol synthesis is discussed.

2. Experimental

2.1. Sample preparation

The oxidic Mo–K/Al_2O_3 sample was prepared by a sequential pore volume impregnation method. γ-Al_2O_3 support (BET surface area 270 $m^2\,g^{-1}$) was first impregnated with K_2CO_3 solution followed by drying at 393 K for 12 h and calcining in air at 573 K for 1 h, and then impregnated with $(NH_4)_6Mo_7O_{24}{\cdot}4H_2O$ solution by drying at 393 K for 12 h and calcining in an oxygen flow of 40 $ml\,min^{-1}$ at 773 K for 24 h. The resulting sample was further calcined in air at 1073 K for 12 h. The Pd-modified samples were prepared by impregnating the obtained Mo–K/Al_2O_3 sample with $PdCl_2$ solutions followed by drying at 393 K for 12 h and calcining in air at 773 K for 2 h. The sulfided samples were obtained by heat-treating the oxidic ones in a flow of CS_2/H_2 mixed gas (8.7% CS_2) of 30 $ml\,min^{-1}$ at 673 K for 6 h. The molybdenum content in the samples, expressed as weight ratio of MoO_3/Al_2O_3, is 0.24, the atomic ratio of K/Mo is 0.8, and the palladium loading varies from 0 to 1.0% of the total weight of the samples.

2.2. Characterization methods

The patterns of X-ray diffraction (XRD) were obtained on a D/MAX-γA rotatory target diffractometer using Cu K_α radiation ($\lambda = 0.15418$ nm, 40 kV and 100 mA). The samples were ground into fine powder and packed into sample holders for measurements.

Laser Raman spectra (LRS) were recorded on an SPEX-1403 spectrometer with a resolution of 2 cm^{-1} using the 488.0 nm^{-1} radiation line from a Spectra-Physics-2020 argon laser. The laser beam intensity and the spectrum slit width were 100 mW and 3.5 cm^{-1}, respectively. The samples were pressed into pellets for the measurements.

The spectra of extended X-ray absorption fine structure (EXAFS) were measured at the beamline of 4WIB of Beijing Synchrotron Radiation Facility (BSRF). The storage ring was operated at 2.2 GeV with a typical current of 50 mA. The fixed-exit Si(111) flat double crystals were used as monochromator. The spectra were recorded in transmission mode with ionization chambers filled with argon. Data analysis was performed following a standard procedure [12]. Phase shifts and backscattering amplitudes extracted from the spectra of $Na_2MoO_4{\cdot}2H_2O$ and MoS_2 standard compounds were used to calculate the structural parameters of the samples.

2.3. Measurements of catalytic activities

The catalytic activities of the sulfided Pd–Mo–K/Al_2O_3 samples for the mixed alcohol synthesis from synthesis gas were measured with a fixed-bed reactor equipped with an on-line gas chromatograph. For each experiment, 0.5 ml of sample was charged into a stainless-steel reactor with inner diameter of 6 mm. The synthesis gas was composed of CO (30%), H_2 (60%) and N_2 (10%). The effluent gas was cooled to 273 K and separated into gas and liquid phases at high pressure. The gaseous products were directly analyzed on a chromatograph through a sampling valve, and the liquid ones were collected for a proper period with their volume and weight measured and subsequently analyzed on the same chromatograph by injection. CO, CO_2 and H_2 in the gas phase and H_2O in liquid products were analyzed on a 2 m TDX-01 column by using a thermal conductivity detector with argon as carrier gas. The hydrocarbons, alcohols and other oxygenated compounds were analyzed on a 2 m Porapak Q column by using a hydrogen flame detector with N_2 as carrier gas. The composition of hydrocarbons was calculated using 1.04% CH_4 as standard gas, while that of the mixed alcohols was calculated directly from the peak areas by using a standard liquid of mixed alcohols. Under the present experimental conditions, since the thermal conductivity detector could detect only a trace amount of CO_2, the activity mentioned below would be referred to as CO_2 free.

3. Results

3.1. XRD

The XRD patterns of the oxidic samples are shown in figure 1. The γ-Al_2O_3 support gives rise to the peaks at d value of 0.239, 0.198, and 0.139 nm. The pattern of the Pd-free sample exhibits the peaks of different K–Mo–O species (figure 1(a)). The strong peaks at d values of 0.396, 0.277, and 0.195 nm may be attributed to the species related to $K_{0.85}Mo_6O_{17}$, as determined by the standard diffraction data from JCPDS cards. This species also has the peaks occurred at d values of 0.328, 0.239, 0.175, 0.159, 0.144, and 0.138 nm. The other weak peaks may result from several kinds of $K_xMo_yO_z$ species ($y = 3, 4, 7$) formed on the support due to the calcination of the samples at high temperature of 1073 K. It is important to note that the main species formed on the support, as determined from the peak intensities, is $K_{0.85}Mo_6O_{17}$. For the Pd-modified samples (figure 1 (b) and (c)), all the peaks arising from K–Mo–O species decrease. No peaks related to the palladium species can be detected.

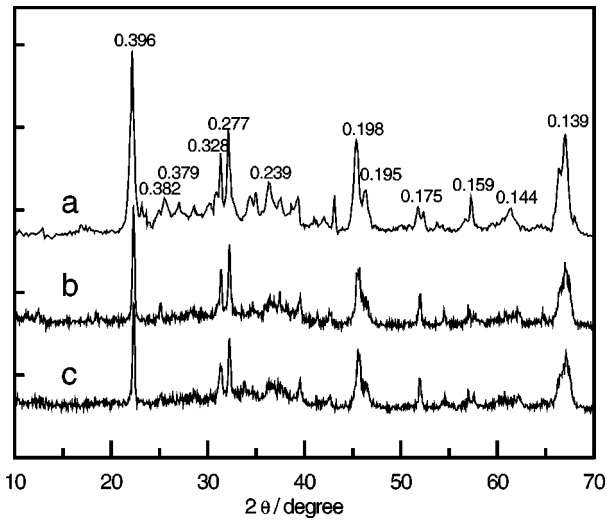

Figure 1. The XRD patterns of oxidic Pd–Mo–K/γ-Al_2O_3 samples with different Pd loadings: (a) 0, (b) 0.5, and (c) 1.0%.

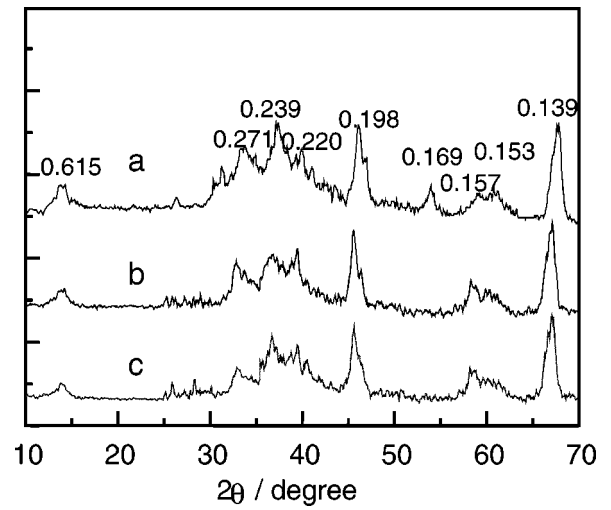

Figure 2. The XRD patterns of sulfided Pd–Mo–K/γ-Al_2O_3 samples with different Pd loadings: (a) 0, (b) 0.5, and (c) 1.0%.

After sulfidation, the diffractions of the K–Mo–O species observed for the oxidic samples are removed (figure 2). Besides the strong peaks arising from the support (0.239, 0.198, and 0.139 nm), very weak broad features can be found at d values of about 0.615, 0.271, 0.236, 0.220, 0.157, and 0.153 nm, indicating the evolution of the poorly crystallized MoS_2. The other species may be assigned to like $K_{0.4}MoS_2$ (0.236, 0.271, 0.157 nm) and K_2MoS_4 (0.345, 0.296, 0.169 nm). However, in the Pd-containing samples, such diffraction peaks as that of $K_{0.4}MoS_2$ and K_2MoS_4 disappear, and the peaks of MoS_2 become broader and weaker, which indicates much smaller MoS_2 crystallite size.

3.2. LRS

LRS of the oxidic samples are presented in figure 3. The spectrum of the Al_2O_3 support is essentially featureless in the region of 100–1100 cm^{-1} under study. The supported oxo-molybdenum species on the oxidic palladium-free sample give rise to several bands in this region (figure 2(a)). Due to the interaction of molybdenum species with the potassium component, the bands typical of bulk MoO_3 (e.g., 818 and 996 cm^{-1}) are absent [13]. According to the literature [14] and previous work performed in our laboratory [13], the bands appearing at 948 and 896 cm^{-1} can be assigned to the octahedrally and tetrahedrally coordinated surface oxo-molybdenum species (Mo(Oh) and Mo(Td)), respectively. The bands occurring at 933, 906, and 352 cm^{-1} correspond to the symmetric stretching, asymmetric stretching and bending vibrations of the terminal Mo=O bond in the octahedrally coordinated MoO_6 species of polymolybdate phases (e.g., $K_{0.85}Mo_6O_{17}$, as revealed by XRD). The bands at 558 and 220 cm^{-1} are due to the symmetric stretching and deformation vibrations of Mo–O–Mo in the MoO_6 unit. In addition, two bands at 1000 and 378 cm^{-1} are characteristic of $Al_2(MoO_4)_3$, a species resulting from the strong interaction of the molybdenum with the support [13].

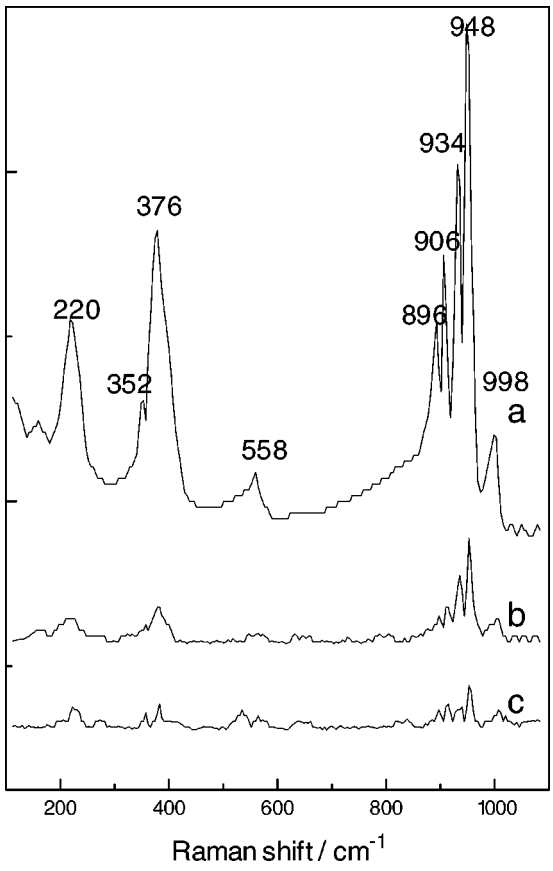

Figure 3. The LRS patterns of oxidic Pd–Mo–K/γ-Al_2O_3 samples with different Pd loadings: (a) 0, (b) 0.5, and (c) 1.0%.

In comparison with the spectrum of the Pd-free sample, the band intensities of the Pd-modified samples remarkably decrease with increasing the palladium loading, but no new band is observed (figure 3 (b) and (c)). It suggests that the sizes of original K–Mo–O species, due to the interaction between palladium and K–Mo species, become much smaller.

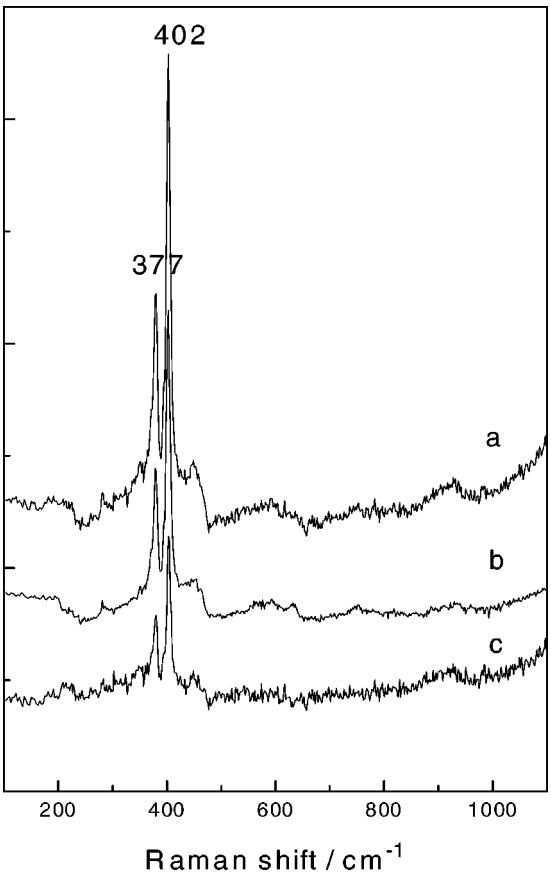

Figure 4. The LRS patterns of sulfided Pd–Mo–K/γ-Al_2O_3 samples with different Pd loadings: (a) 0, (b) 0.5, and (c) 1.0%.

After sulfidation, the oxo-molybdenum species observed for the oxidic samples are not detected, as indicated by the absence of the corresponding bands (figure 4). For the palladium-free sample, the bands at 377 and 402 cm^{-1}, characteristic of MoS_2, are observed [13]. With the incorporation of palladium into the samples, the band intensities of the MoS_2 species decrease due to the interaction of palladium with the sulfided molybdenum species (figure 4 (b) and (c)).

3.3. EXAFS

The magnitude of the Fourier transforms (k^3, $\Delta k = 17$–151 nm^{-1}) of the samples together with the MoS_2 standard compound are shown in figure 5. MoS_2 is of hexagonal structure with one molybdenum atom surrounded by six sulfur atoms at a distance of 0.241 nm and six molybdenum neighbors at 0.316 nm. In the Fourier transforms of the samples (figure 5 (b)–(d)), mainly, two peaks are observed at 0.201 and 0.283 nm. They are located almost at the same positions as those for the MoS_2 standard compound (figure 5(a)), indicating that the local structure of the sulfided molybdenum species is similar to that of MoS_2. In comparison with those of MoS_2, however, the magnitudes of Fourier transforms of the Mo–S and Mo–Mo coordinations are significantly decreased and the ratios of the magnitude of Mo–Mo shell to that of Mo–S (mixed with Mo–O) are also lower. The structural parameters obtained from the fitting results of the molybdenum coordination shells for the samples are presented in table 1. For clarity, the crystallographic data, coordination numbers and distances of the $Na_2MoO_4{\cdot}2H_2O$ and MoS_2 standard compounds, which were used to extract the experimental phases and amplitude functions of the samples, are also collected in table 1. The errors for the fitted parameters corrected as described by Stern et al. [15] are estimated to be 20% in coordination number N, 1% in distance R, 10% in Debye–Waller factor $\Delta\sigma^2$, and 10% in ΔE_0. Since the backscattering amplitudes contain an unknown static and thermal disorder and a damping due to photoelectron losses in the shells, the values of the disorder parameter $\Delta\sigma^2$ reported for the samples are given relative to those for the standard compounds. The moderate $\Delta\sigma^2$ values for the Pd-modified samples indicate a locally ordered MoS_2 structure, but obviously a higher

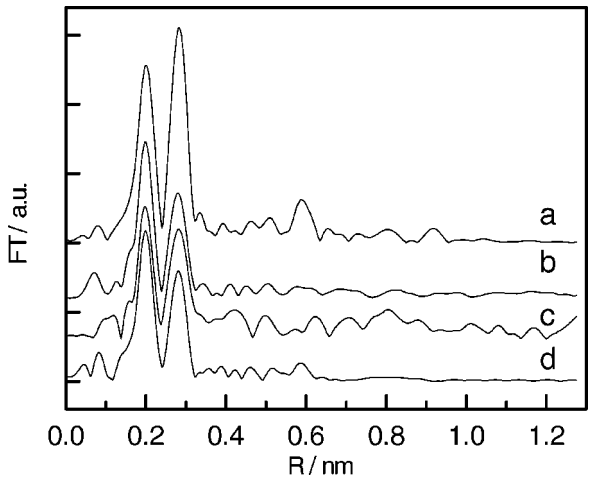

Figure 5. Fourier transforms of $k^3\chi(k)$ for the crystalline MoS_2 and the sulfided samples: (a) MoS_2, (b) Mo–K/Al_2O_3, (c) Pd(0.5%)–Mo–K/Al_2O_3, and (d) Pd(1.0%)–Mo–K/Al_2O_3.

Table 1
Structure parameters from the Fourier-filtered data for the sulfided samples.

Sample	Bond	R (nm)	N	$\Delta\sigma^{2a}$ (10^{-6} nm^2)	$\Delta E_0{}^b$ (eV)
Mo–K/Al_2O_3	Mo–O	0.177	0.2	0	2.43
	Mo–S	0.241	5.1	2	0.65
	Mo–Mo	0.316	3.7	1	1.14
Pd(0.5%)–Mo–K/	Mo–O	0.197	1.2	18	2.84
Al_2O_3	Mo–S	0.243	5.2	11	−1.25
	Mo–Mo	0.315	3.1	11	1.01
Pd(1.0%)–Mo–K/	Mo–O	0.200	1.5	60	−13.4
Al_2O_3	Mo–S	0.243	4.5	20	−0.54
	Mo–Mo	0.315	2.9	24	0.32
$Na_2MoO_4{\cdot}2H_2O$	Mo–O	0.177	4.0		
MoS_2	Mo–S	0.241	6.0		
	Mo–Mo	0.316	6.0		

[a] Relative Debye–Waller factor of the sample to that of the standard compounds.
[b] Correction of the inner-potentials of the samples based upon those of the crystalline MoS_2 compound.

Table 2
Performance of alcohol synthesis over sulfided Pd–Mo–K/Al_2O_3 samples.[a]

Sample (Pd wt%)	CO conversion (%)	Alcohol selectivity[b] (%)	C_nOH selectivity[b] (%)				Ratio[c] MeOH/$C_{2+}OH$	Alcohol STY[d] ($ml\,l^{-1}\,h^{-1}$)
			MeOH	EtOH	PrOH	BuOH		
0	4.9	33.4	14.8	13.6	4.3	0.7	0.80	28.8
0.5	7.2	34.7	11.9	14.2	7.7	0.9	0.53	38.4
1.0	8.4	40.2	13.5	15.3	9.4	2.0	0.50	49.8

[a] Reaction conditions: 623 K, 5.0 MPa, 4800 h^{-1}, $H_2/CO = 2$ (v/v).
[b] Selectivity is the percentage of moles of CO converted into alcohols on a CO_2-free basis.
[c] Ratio is the carbon number of methanol to that of higher alcohols.
[d] STY is the space–time yield for alcohols in milliliter of alcohols produced per liter of catalyst per hour.

disorder than that for the MoS_2 standard compound due to the decrease in the average particle size of MoS_2 slabs in the samples.

3.4. Performance of the samples used for alcohol synthesis

The data in table 2 show the influence of incorporation of Pd promoter to the sulfided K–Mo/Al_2O_3 sample on the catalytic features for the synthesis of mixed alcohols from syngas. Over the Pd-free sample the activity toward alcohol formation is rather low, methanol being the main product. With palladium modified, the activity for alcohol formation is remarkably increased without noticeable increase of hydrocarbon yields. Another obvious change is that the alcohol ratios of C_1/C_{2+} in the products for palladium-promoted samples decrease notably relative to that for the unpromoted sample. It suggests that the incorporation of palladium into the sample promote the conversion of synthesis gas to higher alcohols.

4. Discussion

The results of XRD, LRS and EXAFS reveal that the molybdenum species in the sulfided samples mainly exist in the form of MoS_2-like crystallites (figures 2, 4, and 5). Topsøe et al. [16] claimed that the MoS_2 crystallites supported on alumina can be present as large patches of a wrinkled, one slab thick MoS_2-like layer, which are stabilized through the weak van der Waals interaction of the basal planes of MoS_2 particles with the surface of the support. For the sulfided sample free of palladium, it might be the case, since the size of the slabs is rather large, as indicated by the Mo–Mo coordination numbers (table 1).

For the Pd-modified samples, just as we found in the sulfided Rh–Mo–K/Al_2O_3 catalysts [17], the formed MoS_2 crystallites may be small enough to interact with the support with their basal planes oriented perpendicular to the support surface. This point may also be interpreted by the fact that the contribution of Mo–O coordination is increased with increasing the palladium loading (table 1). Based upon the suggestion of Prins et al. [18], the supported oxo-molybdenum species should be fully sulfided under the present conditions used for the sulfidation of the catalysts. In such a case, the contribution of Mo–O coordination observed for the samples may not arise from the oxygen atoms merely connected to molybdenum atoms due to the incomplete sulfidation of the samples, but from the interaction of the molybdenum atoms with the surface oxygen atoms of the alumina support, i.e., from the bonding of Mo–O–Al. If the sulfided molybdenum species interact with the support through their basal planes, instead of the edge planes, the average Mo–S coordination would not change much with decreasing slab size and the contribution of Mo–O coordination would not be so pronounced (table 1). Therefore, the MoS_2-like crystallites are present as thin, hexagonally shaped slabs with truncated edges. The high-energy edge planes contacting the gas phase, presumably active in the catalytic reactions of alcohol synthesis, can be assigned as the $(10\bar{1}0)$ set of planes, while the truncated edge planes bonded to the surface of alumina are assigned as the $(2\bar{1}\bar{1}0)$ planes due to the finest geometrical fit with the most stable surface of alumina (110) [17]. Since the sizes of the sulfided molybdenum species in the sample may not be uniform, the small crystallites in the palladium-free sample may also be stabilized through the bonding of Mo–O–Al which gives rise to the minor contribution of Mo–O coordination as shown in table 1.

On the other hand, many authors proposed that the catalytic active sites on sulfided molybdenum-based catalysts are due to the so-called coordinately unsaturated molybdenum (Mo(CUS)) sites, on which chemisorption of probe molecules can occur [19,20]. They are formed on the surface of MoS_2 crystallites during sulfidation or even induced by the stream of the reactants. At a reaction temperature of 573 K, H_2 molecules adsorbed on the Mo(CUS) sites possibly dissociate and then, by spillover or other ways, migrate to the basal planes of the MoS_2 crystallites, where they bond with sulfur atoms to form SH species. A multilayer growth of MoS_2 crystallites perpendicular to the basal planes is unfavorable to H_2 adsorption. For the oxidic Pd–Mo–K/Al_2O_3 samples, the XRD and LRS results clearly demonstrate that the incorporation of palladium improves the dispersion of the oxo-molybdenum species (figures 1 and 3). The sulfidation of the species gives rise to a dispersion of the supported MoS_2 crystallites higher than that in the palladium-free sample as revealed also by LRS and EXAFS results (figures 4 and 5). Accordingly, the average

size of the MoS_2 crystallites is reduced, which will facilitate the creation of Mo(CUS) sites. In addition, as a result of the reduction in the size of the MoS_2 crystallites, the migration of the adsorbed H_2 molecules from the Mo(CUS) sites to the MoS_2 surface to form the SH species becomes easier, which may be responsible for the high selectivity to the formation of C_{2+} alcohols (table 2).

The dispersion of the incorporated palladium species may also be an important issue related to the properties of the catalysts for alcohol synthesis. As mentioned above, however, no XRD peaks arising from the palladium species incorporated into the Mo–K/Al_2O_3 samples are observed. It suggests that the palladium aggregation might be suppressed by the interaction between the palladium and K–Mo species. As shown in table 2, the yield of hydrocarbons over the Pd–Mo–K/Al_2O_3 samples is lower than that obtained with the palladium-free sample. It may also indicate that the supported palladium species are highly dispersed since the formation of hydrocarbons needs large palladium clusters. Lunsford et al. [17] concluded that Pd structural effects play an important role in the activity of the catalyst, since catalysts with small Pd crystallites produce methanol while larger crystallites produce methane. From another point of view, taking a page from conventional NiMo and CoMo catalyst theory [21], one might blame the activity and selectivity properties of the Pd-containing materials on special "Pd–S–Mo" sites. The active phase could be described as consisting of small MoS_2 particles with Pd promoter atoms decorating the edges of the MoS_2 slabs. The role of the MoS_2 particles is to act as a secondary support merely to stabilize the highly dispersed Pd sulfide located on the edges. Stabilization of the MoS_2 slabs themselves is assumed to occur via Mo–O linkages to the support, as proposed by several authors (just as discussed above). Therefore, the high dispersion of the palladium species caused by the Pd–Mo interaction may also be an important factor that is responsible for the formation of alcohols.

5. Conclusions

With the incorporation of palladium into the oxidic Mo–K/Al_2O_3 samples, a strong interaction of the palladium modifier with the oxo-molybdenum components occurs, which gives higher dispersion of molybdenum species on alumina. After sulfidation of the samples, the Pd-promoted samples show much smaller MoS_2 size as compared with the Pd-free sample. The sulfided molybdenum species in the palladium-free sample are present as large patches of MoS_2-like slabs that may be oriented with their basal planes parallel to the surface of the support. With the modification of palladium to the catalysts, the sulfided molybdenum species become highly dispersed. The interaction of the palladium with the molybdenum species may cause the basal planes of the MoS_2-like species to become oriented perpendicular to the support surface due to the favorable bonding between the MoS_2 edge planes and the support.

The activity for alcohol synthesis over the Pd-modified catalysts is much higher than that obtained over the Pd-free one and increases with increasing the palladium loading, which may result from the appearance of the more catalytically active surfaces or sites modified by the palladium species. The high selectivity to the formation of C_{2+} alcohols obtained with the palladium-modified samples is most probably due to the interaction between the palladium and the molybdenum species.

Acknowledgement

This work was supported by National Natural Science Foundation of China (No. 29773042). The experimental facility of EXAFS was supplied by BSRF.

References

[1] C.N. Satterfield, *Heterogeneous Catalysis in Industrial Practices*, 2nd Ed. (McGraw-Hill, New York, 1991) p. 454.
[2] H.H. Kung, Catal. Rev. 22 (1980) 235.
[3] K. Klier, in: *Catalysis of Organic Reactions*, ed. W.R. Moser (Dekker, New York, 1981) p. 195.
[4] K. Klier, in: *Advance in Catalysis*, Vol. 31, eds. D.D. Eley, H. Pines and P.B. Weiss (Academic Press, New York, 1982) p. 243.
[5] M. Ichikawa, Bull. Chem. Soc. Jpn. 51 (1978) 2268.
[6] J.M. Driessen, E.K. Poels, J.P. Hindermann and V. Ponec, J. Catal. 82 (1983) 26.
[7] F. Fajula, R.G. Anthony and J.H. Lunsford, J. Catal. 73 (1982) 237.
[8] E.K. Poels, E.H. van Broekhoven, A.A. van Barneveld and V. Ponec, React. Kinet. Catal. Lett. 18 (1981) 223.
[9] T. Tatsumi, T. Uematsu and J.H. Lunsford, in: *Abstracts, 8th North American Meeting of the Catalysis Society*, Philadelphia, 1–4 May 1983.
[10] Yu.I. Ryndin, R.F. Hicks, A.T. Bell and Yu.I. Yermakov, J. Catal. 70 (1981) 287.
[11] G.Z. Bian, Y.L. Fu and Yamada, Appl. Catal. A 144 (1996) 79.
[12] D.E. Sayers and B.A. Bunker, in: *X-Ray Absorption, Principles, Applications, Techniques of EXAFS, SEXAFS and XANES*, eds. D.C. Koningsberger and R. Prins (Wiley, New York, 1988) p. 211.
[13] M. Jiang, G.Z. Bian and Y.L. Fu, J. Catal. 146 (1994) 144.
[14] G.L. Schrader and C.P. Cheng, J. Catal. 80 (1983) 369.
[15] E. Stern, M. Newville, B. Ravel, Y. Yacoby and D. Haskel, Physica B 208/209 (1995) 117.
[16] H. Topsøe and B.S. Clausen, Catal. Rev. Sci. Eng. 26 (1984) 395.
[17] Z. Li, M. Jiang, G. Bian, Y. Fu and S. Wei, J. Synchrotron Rad. 6 (1999) 462.
[18] R. Prins, V.H.J. De Beer and G.A. Somorjai, Catal. Rev. Sci. 31 (1989) 1.
[19] J. Valyon and W.K. Hall, J. Catal. 84 (1983) 216.
[20] M.I. Zaki, B. Vielhaber and H. Knoezinger, J. Phys. Chem. 90 (1986) 3176.
[21] H. Topsøe, B.S. Clausen, N.Y. Topsøe and E. Pedersen, Ind. Eng. Chem. Fund. 25 (1986) 25.